J Wood Sci (2012) 58:453–458
DOI 10.1007/s10086-012-1266-6

NOTE

Examination of the failure behavior of wood with a short crack in the radial–longitudinal system by single-edge-notched bending test

Tetsuya Nakao · Cicilia Maria Erna Susanti · Hiroshi Yoshihara

Received: 11 January 2012 / Accepted: 11 April 2012 / Published online: 26 April 2012

Abstract The failure behavior of wood with a short crack was examined by conducting the single-edge-notched bending tests of a radial-longitudinal system on Agathis specimens. In the test, the mode I critical stress intensity factor was measured, and its validity was checked by the result from double cantilever beam testing method. The mode I critical stress intensity factor decreased when the crack length approached zero. With crack length correction, a constant critical stress intensity factor was obtained over a wide range of crack length including crack-free specimen.

Keywords Single-edge-notched bending test · Mode I stress intensity factor · Bending strength · Correction crack length

Introduction

In actual cases as timber engineering and wood drying, the crack lengths in wood are often short. In a previous study [1], the single-edge-notched bending (SENB) tests of tangential–radial (TR) system were conducted using specimens of Agathis (*Agathis* sp.) with varying the crack lengths that were smaller than those adopted in several existing studies involving the single-edge-notched tension or bending tests [2–8]. When considering an additional crack length ahead of the crack tip, the mode I critical stress intensity factor was effectively predicted independently from the initial crack length. In addition, the nominal bending strength could also be predicted in both cases of with and without a crack based on the concept for the additional crack length.

In practical operations such as timber engineering and drying, a crack induced in solid wood often propagates along the fiber, so it is important to investigate whether the concept described above is valid for the system including the fiber direction. In this study, the radial–longitudinal (RL) system SENB tests were conducted, and the validity of the results was examined by comparing test data with those obtained from double cantilever beam (DCB) tests.

T. Nakao (✉) · C. M. E. Susanti · H. Yoshihara
Faculty of Science and Engineering, Shimane University, Nishikawazu-cho 1060, Matsue, Shimane 690-8504, Japan
e-mail: nakaote@riko.shimane-u.ac.jp

Theory

Three-point SENB test analyses

Figure 1 shows a schematic diagram of the three-point SENB test. The specimen which had a crack of length a at its center was supported with a span of S, and the load P was applied at the mid-span. The initial crack length is defined as a. In this loading condition, the nominal bending stress σ_n is derived from the elementary beam theory as follows:

$$\sigma_n = \frac{3SP}{2BW^2}, \quad (1)$$

where B and W are the beam width and depth, respectively. This notation is applicable to crack-free specimens. When a crack-free specimen is bent, the failure-by-bending moment is induced when σ_n reaches its critical value σ_{nc}, which is usually defined as the bending strength of the material.

The fracture behavior of a material with a long crack should be analyzed using the mode I stress intensity factor

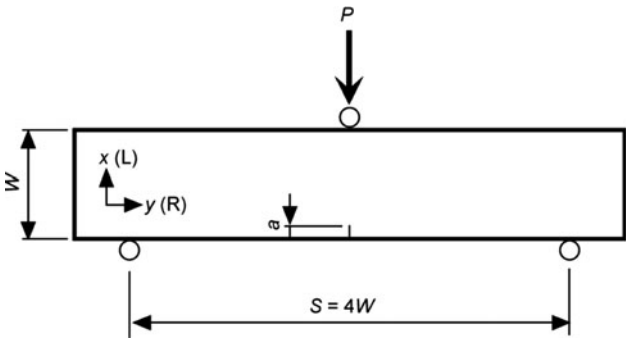

Fig. 1 Schematic diagram of the three-point single-edge-notched bending (SENB) test

K_I or the energy release rate G_I, each of which is derived from fracture mechanics theory. In SENB testing of specimens with a short crack, however, it is difficult to measure G_I appropriately, because the loading-line compliance does not vary with the crack length [1]. In contrast, K_I is more easily measured using an approximating equation.

The mode I stress intensity factor K_I is derived using the following equation:

$$K_I = \sigma_n \sqrt{\pi a} f\left(\frac{a}{W}\right), \tag{2}$$

where $f(a/W)$ is the crack geometry factor. The fracture is initiated when K_I reaches the critical stress intensity factor, defined as K_{Ic}, which is obtained by substituting σ_{nc} for σ_n in Eq. (2). Gross and Srawley derived a $f(a/W)$–a/W relationship for isotropic material as follows [9]:

$$f\left(\frac{a}{W}\right) = 1.09 - 1.735\left(\frac{a}{W}\right) + 8.20\left(\frac{a}{W}\right)^2 - 14.18\left(\frac{a}{W}\right)^3 + 14.57\left(\frac{a}{W}\right)^4. \tag{3}$$

There was a concern that the orthotropy of the wood might influence the crack geometry factor. However, Eq. (3) was appropriate as the crack geometry factor for the TR system SENB specimens with the configuration similar to this study according to the virtual crack closure technique (VCCT) applied to the results obtained from the finite element analyses [1]. Moreover, the validity of Eq. (3) was verified for wood with a strong orthotropy, such as TL system fracture mechanics testing analyses [10]. Hereafter, the mode I stress intensity factor is calculated using the crack geometry factor represented by Eq. (3).

Double cantilever beam test analyses

Double cantilever beam test in the RL system (Fig. 2) was conducted to examine the validity of SENB testing results. According to beam theory and fracture mechanics, the mode I energy release rate can be obtained as follows [11]:

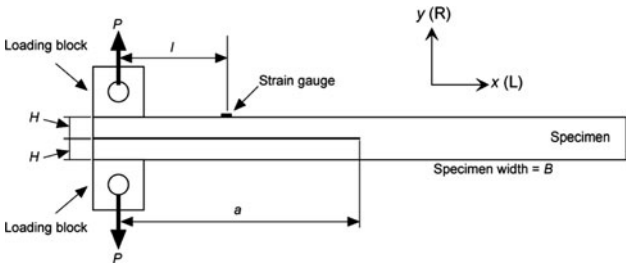

Fig. 2 Schematic diagram of double cantilever bending (DCB) test

$$G_I = \frac{3P^2 C_L}{2B}\left(\frac{3Hl}{4}\cdot\frac{C_L}{C_S}\right)^{-\frac{1}{3}} \tag{4}$$

where C_L is the compliance obtained from the load–deflection relationship, and C_s is the compliance obtained from the load–longitudinal strain relationship, which was measured at $l = a/2$.

Here, the energy release rate was converted to the stress intensity factors as follows:

$$K_I = \sqrt{\frac{E_x G_I}{c_I}}, \tag{5}$$

where

$$c_I = \frac{1}{\sqrt{2}}\sqrt{\frac{E_x}{E_y}}\sqrt{\sqrt{\frac{E_x}{E_y}} + \frac{1}{2}\left(\frac{E_x}{G_{xy}} - 2\nu_{xy}\right)} \tag{6}$$

in which E_x and E_y are Young's moduli in the x and y directions, respectively, and G_{xy} and ν_{xy} are the shear modulus and Poisson's ratio in the xy plane, respectively [12]. In this study, xy plane denotes RL plane. The elastic modulus values were obtained by compression tests and vibration tests [1], and are listed in Table 1.

Experimental

Materials

Agathis (*Agathis* sp.) lumber, with a density of 480 ± 10 kg/m^3 at 12 % moisture content (MC), was used for the tests. When examining the fracture mechanics properties of the radial–longitudinal system, the influence of the annual rings is often significant [8]. Agathis is a tropical wood species with no significant growth rings;

Table 1 Elastic constants used for the conversion to stress intensity factor

E_x (GPa)	E_y (GPa)	G_{xy} (GPa)	ν_{xy}
14.6	0.87	1.0	0.44

x and y directions correspond to the longitudinal and radial directions of wood, respectively

hence, the influence of annual rings could be ignored in the analysis. The lumber had no defects such as knots or grain distortions, so that the specimens cut from it could be regarded as small and clear. The lumber was stored for several months in a room at a constant temperature of 20 °C and a relative humidity of 65 % before the test and was confirmed to be in an air-dried condition. These conditions were maintained throughout the tests. The equilibrium MC was approximately 12 %.

Single-edge-notched bending tests

All of the specimens were cut from the lumber described above so that they were long-matched to the dimensions shown in Table 2. The numbers of specimens were 50, 25, and 15 for specimen A, B, and C, respectively. For the cracked specimens, a crack was produced along the radial direction in the RL system. The crack was first cut with a band saw (thickness = 1 mm), it was then extended ahead of the crack tip using a razor blade. The specimen was supported by the span shown in Table 2, and a load was applied to the specimen at a crosshead speed of 1 mm/min for the test with span lengths of 60 and 120 mm, a crosshead speed of 2 mm/min was used for the test with a span length of 240 mm. The test was conducted until the load markedly decreased.

Figure 3 shows a typical load–loading-line deflection relation obtained by the SENB test. The load increases linearly until it is maximum, and then drops immediately without displaying a nonlinear phase. This trend is similar to that obtained from the SENB tests of the specimen with the TR system [1]. In this research, the critical load for crack propagation P_c was determined as the maximum load, as the same manner with that in the previous study [1]. By substituting P_c into Eq. (1), the nominal bending strength σ_{nc} corresponding to initial crack length a was obtained [1]. Then, the mode I critical stress intensity factor K_{Ic} corresponding to the initial crack length was obtained by substituting σ_{nc} and $f(a/W)$ represented as Eq. (3) into Eq. (2).

Double cantilever beam test

All of the specimens were cut from the lumber mentioned above so that they were side matched into the initial dimensions of 30 mm (radial direction) × 15 mm (tangential direction) × 315 mm (longitudinal direction). The number of specimens was six. The crack was first cut along the longitudinal direction in the longitudinal–radial plane with a band saw (thickness = 1 mm), and then it was extended 1 mm ahead of the crack tip using a razor blade so that the crack length would be as that mentioned below. After cutting the crack, the loading blocks of MDF with the dimensions of 30 mm in length, 30 mm in height, and 15 mm in thickness were bonded by epoxy resin on the upper and lower cantilever portions symmetrically as shown in Fig. 2. Crack length, which was defined as the distance from the line of load application to the crack tip, was 150 mm. Load P was applied to the specimen by pins through universal joints at a crosshead speed of 5 mm/min until the load markedly decreased. The total testing time was about 10 min.

The loading-line displacement δ was measured by the crosshead travel since it was confirmed that the machine compliance was small enough to be ignored [7], whereas the longitudinal strain ε was measured by a strain gauge (gauge length = 2 mm; FLA-2-11, Tokyo Sokki Co., Tokyo) bonded at the midpoint between the loading line and crack tip on the top cantilever portion ($l = a/2$). The C_L and C_S values were obtained from the linear portions of P–δ and P–ε relationships, respectively [11]. The critical load for crack propagation P_c was defined as that at the onset of nonlinearity in the load–loading-line displacement curve [7, 13, 14].

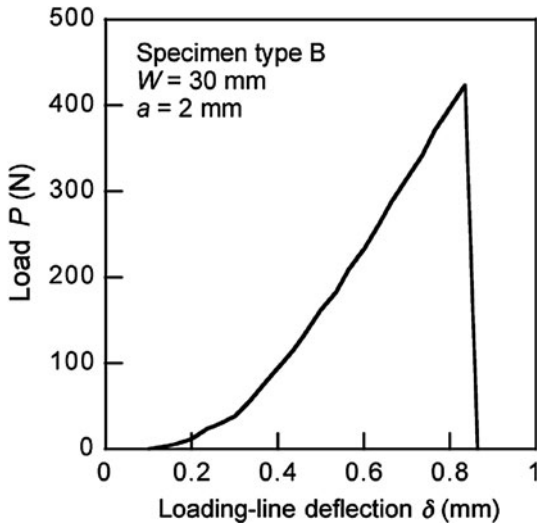

Fig. 3 Typical example of the load–loading-line deflection relation by the SENB test

Table 2 Specimen configurations used for the SENB tests

Specimen type	Span S (mm)	Depth W (mm)	Width B (mm)	Crack length a (mm)
A	60	15	7.5	0, 0.5, 1, 2, 4
B	120	30	15	0, 0.5, 1, 2, 4
C	240	60	30	0, 0.5, 1, 2, 4

Results and discussion

Three-point SENB test

Figure 4 shows the relationship between the nominal bending strength σ_{nc} and initial crack length a. According to the results for metals [15, 16], the nominal bending strength of a cracked specimen will approach the bending strength of a crack-free

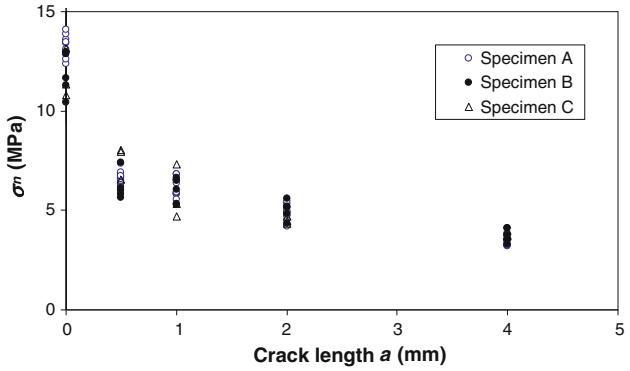

Fig. 4 Relationship between the nominal bending strength σ_{nc} and crack length a by the SENB test

specimen when the crack length is decreased. From the results obtained here, however, the value of σ_{nc} is markedly smaller than that of the crack-free specimen, and it decreases as the crack length increases. This tendency is similar to that for the results obtained using the specimens with the TR system [1], and it suggests that fracture mechanics theory is essential for analyzing the failure behavior of solid wood with a crack even when the crack length is short.

Figure 5 shows the relationship between the mode I critical stress intensity factor K_{Ic} and the initial crack length a. The K_{Ic} value obtained by the DCB test, the details of which are mentioned below, is also shown in Fig. 5. The K_{Ic} value can be regarded to be a material parameter independently determined from the initial crack length. Nevertheless, the K_{Ic} value is not constant and it significantly increases as the initial crack length increases.

The dependence of K_{Ic} value on the initial crack length a can be reduced by introducing an additional crack length Δ into Eq. (2) [1, 17]:

$$K_I = \sigma_n \sqrt{\pi(a+\Delta)} f\left(\frac{a+\Delta}{W}\right) = \sigma_n \sqrt{\pi a'} f\left(\frac{a'}{W}\right), \qquad (7)$$

where a' is defined as the corrected crack length. Table 3 shows the value of the additional crack length Δ corresponding to each specimen type. The value of Δ was determined as follows: (1) the values of K_{Ic} were calculated under various values of Δ in Eq. (7), (2) the standard deviations of K_{Ic} corresponding to each crack length were obtained, (3) the sums of the standard deviations, defined as s_D, corresponding to each Δ were obtained and compared. The value of Δ in Table 3 was determined as that from which the smallest value of s_D was derived. Figure 6 shows the relationship between the mode I critical stress intensity factor K_{Ic} and the corrected crack length a'. By conducting the crack length correction, the dependence of K_{Ic} on the crack length is effectively reduced. The concept for introducing the additional crack length is also applicable for the crack-free specimen. Although the dimensions of the specimens vary significantly, the variation of the additional crack length values is relatively small. These additional crack length values are similar to those obtained from the tests of the specimens with the TR system [1]. In a previous study, we examined the mode II fracture behavior of Agathis by asymmetric four-point bending tests of a specimen with a short crack in the TL system, which were cut from the same lumber used in this investigation [17]. The test results were analyzed with the same manner conducted here, and we found that the additional crack length values obtained in this study are shorter than that obtained from the mode II tests [17]. Table 4 shows the average values of K_{Ic} obtained with and without correcting the crack length.

The relationships between σ_{nc} and a can be conventionally predicted by substituting the values of K_{Ic} without

Table 3 Additional crack length corresponding to each specimen type

Specimen type	Additional crack length Δ (mm)
A	0.25
B	0.33
C	0.33

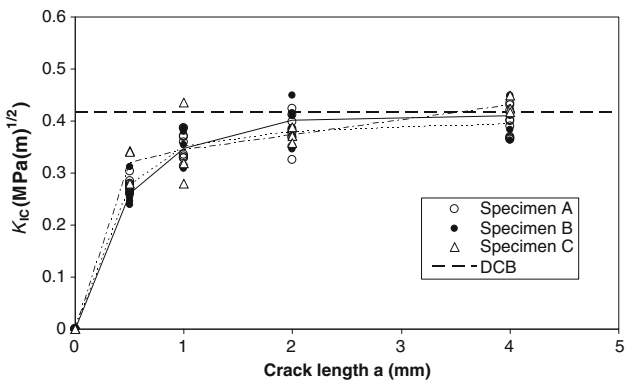

Fig. 5 Relationship between the mode I critical stress intensity factor K_{Ic} and crack length a

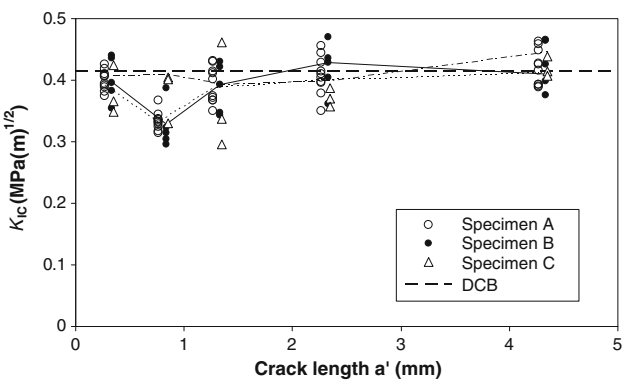

Fig. 6 Relationship between the mode I critical stress intensity factor K_{Ic} and corrected crack length a'

Table 4 Mode I critical stress intensity factor K_{Ic} obtained with and without correcting the crack length

Specimen type	K_{Ic} (MPa $m^{1/2}$)	
	Crack length uncorrected	Crack length corrected
A	0.35 ± 0.052(a)	0.38 ± 0.037(b)
B	0.36 ± 0.069(a)	0.39 ± 0.051(b)
C	0.37 ± 0.058(a)	0.41 ± 0.047(b)

Results are averages ± SD. The K_{Ic} values listed are obtained by averaging the values corresponding to the initial crack length a of 0.5, 1, 2, 3, and 4 mm in (a), and $a = 0$, 0.5, 1, 2, 3, and 4 mm in (b)

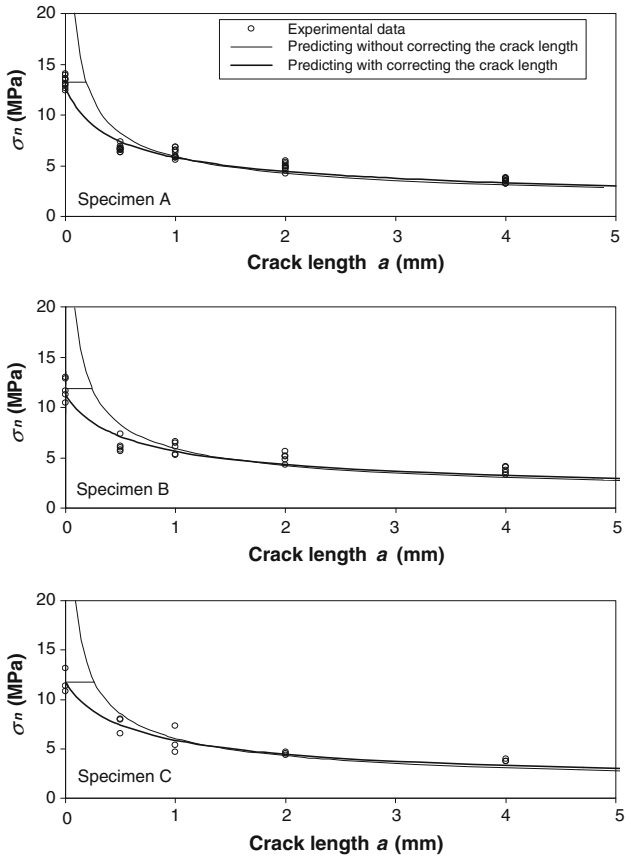

Fig. 7 Comparison of nominal bending strengths experimentally obtained and predicted on the basis of fracture mechanics theory

the crack length correction in Table 4 and $f(a/W)$ into Eq. (2) [15]. In addition, the σ_{nc}–a relationships are also predicted by substituting the values of K_{Ic} with the crack length correction in Table 4, Δ in Table 3, and $f((a + \Delta)/W)$ into Eq. (7). This method is our proposal. Figure 7 compares the predicted and experimentally obtained σ_{nc}–a relationships. When the crack length is not corrected, the predicted strength increases markedly when the crack length approaches zero. When the crack length is corrected, however, the σ_{nc}–a relationship is effectively predicted over the full range of crack lengths, including when $a = 0$.

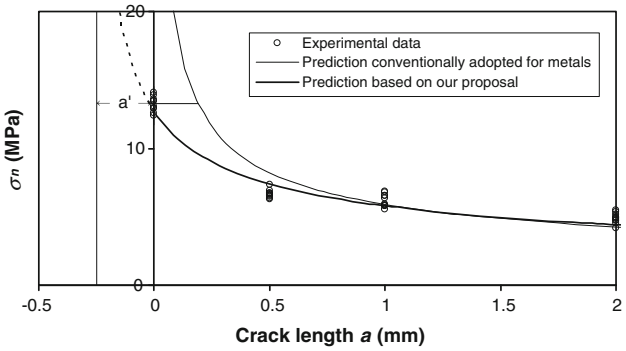

Fig. 8 A relationship between strength and crack length for wood

This is the same result as those in the previous works [1, 17]. Therefore, the failure behavior is probably described by fracture mechanics theory even when the specimen has no crack as shown in Fig. 8 in comparison with the failure behavior of metal [15, 16].

For wood as quasi-brittle material, so-called fracture process zone influence [18–24] might not be so significant because the nonlinearity in the load–loading-line deflection relation is not significant as Fig. 3 shows. Natural cracks inherently contained in wood might be significant to the phenomenon obtained in this study. Further researches including the microscopic observation will reveal this phenomenon.

Comparison with DCB test results

The average K_{Ic} value by DCB test was 0.42 ± 0.02 MPa $m^{1/2}$. The average K_{Ic} values by SENB are 0.35 ± 0.058 MPa $m^{1/2}$ for 0.5–4 mm crack length specimens before correction and 0.39 ± 0.044 MPa $m^{1/2}$ for all specimens including crack-free specimens after additional crack length correction. The results obtained from the SENB tests approached to DCB results after the correction. By the t test between the results obtained from the DCB and SENB tests, the probability value (P value) was 0.011 before correction and the difference was significant at 5 % level. In contrast, the P value was 0.19 after correction, so the difference was not significant at 5 % level. Although the DCB specimens used here were not longitudinally matched to the SENB specimens but were only in the same lumber, the results may show the validity of introducing the additional crack length.

There have been several approaches on the application of fracture mechanics to the crack free specimens [25, 26]. Further researches are required for revealing the failure behavior of solid wood based on our proposal as well as the examinations described above.

Acknowledgments The authors thank Dr. He Wen for his help in conducting the experiment. This study was partly supported by a

Grant-in-Aid for Scientific Research (C) (No. 21580207) of the Japan Society for the Promotion of Science (JSPS).

References

1. Susanti CME, Nakao T, Yoshihara H (2010) Examination of the failure behaviour of wood with a short crack in the tangential-radial system by single-edge-notched bending test. Eng Fract Mech 77:2527–2536
2. Tribourlot P, Jodin P, Pluvinate G (1984) Validity of fracture mechanics concepts applied to wood by finite element calculation. Wood Sci Technol 18:51–58
3. Ashby MF, Eastering KE, Harrysson R (1985) The fracture and toughness of woods. Proc R Soc Lond A 398:261–280
4. Le-Ngoc L, McCallion H (1997) On the fracture toughness of orthotropic materials. Eng Fract Mech 58:355–362
5. Ando K, Ohta M (1999) Variability of fracture toughness by the crack tip position of coniferous wood. J Wood Sci 45:275–283
6. Wang L, Lu Z, Zhao G (2003) Wood fracture pattern during the water adsorption process. Holzforschung 57:639–643
7. Samarasinghe S, Kulasiri D (2004) Stress intensity factor of wood from crack-tip displacement fields obtained from digital image processing. Silva Fennica 38:267–278
8. Watanabe K, Shida S, Ohta M (2011) Evaluation of end-check propagation based on mode I fracture toughness of sugi (*Cryptomeria japonica*). J Wood Sci 57:371–376
9. Gross B, Srawley JE (1965) Stress-intensity factors for three-point bend specimens by boundary collocation. NASA TN D-3092
10. Yoshihara H (2010) Examination of the mode I critical stress intensity factor of wood obtained by single-edge-notched bending test. Holzforschung 64:501–509
11. Yoshihara H, Kawamura T (2006) Mode I fracture toughness estimation of wood by DCB test. Composites A 37:2105–2113
12. Sih GC, Paris PC, Irwin GR (1965) On cracks in rectilinearly anisotropic bodies. Int J Fract Mech 1:189–203
13. Hojo M, Kageyama K, Tanaka K (1995) Prestandardization study on mode I interlaminar fracture toughness test for CFRP in Japan. Composites 26:243–255
14. Brunner AJ, Blackman BRK, Davies P (2001) Mode I delamination. In: Moore DR, Pavan A, Williams JG (eds) Fracture Mechanics Testing Methods for Polymers Adhesives and Composites. ESIS Publication 28. Elsevier, Amsterdam, pp 277–305
15. Irwin GR, Kies JA, Smith HL (1958) Fracture strength relative to onset and arrest of crack propagation. Proc ASTM 58:640–657
16. Leicester RH (2006) Application of linear fracture mechanics to notched timber elements. Prog Struct Eng Mater 8:29–37
17. Susanti CME, Nakao T, Yoshihara H (2011) Examination of the Mode II fracture behaviour of wood with a short crack in an asymmetric four point bending test. Eng Fract Mech 78: 2775–2788
18. Bažant ZP (2002) Concrete fracture model: testing and practice. Eng Fract Mech 69:165–205
19. Morel S, Bouchaud E, Schmittbuhl J (2003) Influence of the specimen geometry on *R*-curve behavior and roughening of fracture surfaces. Int J Fract 121:23–42
20. Morel S, Dourado N, Valentin G, Morais J (2005) Wood: a quasibrittle material *R*-curve behavior and peak load evaluation. Int J Fract 131:385–400
21. Dourado NMM, Morel S, de Moura MFSF, Valentin G, Morais J (2008) Comparison of fracture properties of two wood species through cohesive crack simulations. Composites A 39:415–427
22. de Moura MFSF, Morais JJL, Dourado N (2008) A new data reduction scheme for mode I wood fracture characterization using the double cantilever beam test. Eng Fract Mech 75:3852–3865
23. de Moura MFSF, Campilho RDSG, Gonçalves JPM (2008) Crack equivalent concept applied to the fracture characterization of bonded joints under pure mode I loading. Compos Sci Technol 68:2224–2230
24. de Moura MFSF, Dourado N, Morais JJL (2010) Crack equivalent based method applied to wood fracture characterization using the single edge notched-three point bending test. Eng Fract Mech 77:510–520
25. Masuda M (1986) Theoretical consideration on fracture criteria of wood. Bull Kyoto Univ Forests 58:241–250
26. Ogawa M, Sobue N (1997) Fracture of bolted timber joints with cracks at bolt hole edges. Mokuzai Gakkaishi 43:1002–1008